Characterization of Titanium Oxide Layers Formation Produced by Nanosecond Laser Coloration

CrossMark

F. BRIHMAT-HAMADI, E.H. AMARA, and H. KELLOU

Laser marking technique is used to produce colors on titanium while scanning a metallic sample under normal atmospheric conditions. To proceed with different operating conditions related to the laser beam, the parameters of a Q-switched diode-pumped Nd:YAG (λ = 532 nm) laser, with a pulse duration of τ = 5 ns, are varied. The effect on the resulting mark quality is the aim of the present study which is developed to determine the influence of the operating parameters (*i.e.*, pulse frequency, beam scanning speed, and pumping intensity) and furthermore their combination, such as the accumulated fluences and the overlapping rate of laser impacts. From the obtained experimental results, it is noted that the accumulated fluences and the scanning speed are the most influential operating parameters during laser marking, since they have a strong effect on the surface roughness and reflectance, and the occurrence of many oxide phases such as TiO, Ti_2O_3, TiO_2 (γ- phase, anatase, and rutile).

I. INTRODUCTION

TITANIUM presents interesting physical properties such as high strength, hardness, durability, low density, corrosion resistance, and biological compatibility. It is considered as one of the most suitable materials in laser processing for the use in many advanced applications such as surgery implants,[1–4] aerospace industry, jewelry, *etc*. Laser beams allow the obtaining of higher quality marked items from the point of view of the cleanliness, reproducibility, precision, and reliability. Obtaining colors on laser processed metallic surfaces may be conducted under normal or controlled atmospheric pressure conditions; it is based on the heating of the material surface. The resulting thermal field leads to changes on the metallic surface properties, without significant modifications on the basic material. The obtained colors are the result of surface oxidation, and the colored appearance of oxide films is due to interferences effect of the reflected natural light.[5] It is found in literature that Ti oxide films can be generated by different methods such as heat treatment, cathodic deposition,[6] plasma deposition,[7] pulsed laser deposition,[8] magnetron sputtering,[9] thermal oxidation,[10] electrolytic oxidation (anodizing),[11,12] and laser oxidation.[12–14] Metal coloring by lasers appeared fifteen years ago, and compared to other methods of marking, a wider range of applications is found in practice. The laser technique offers greater accuracy, non-contact working with the surface, reduction in industrial effluents (no acid, solvent), significant cost reduction, fastness, flexibility, high amount of recorded information per unit treated surface, and allows performing films when surface is of complex shape.

The marking process can be optimized for producing colors with better quality and visual appearance by adjusting the processing parameters, mainly related to the laser beam. Laser marking of metallic surfaces with the right parameters creates oxide layers, the thicknesses of which determine the reflection of the natural white light. Under air ambience, titanium is known for its easiness coloration by laser beams. By varying the laser operating parameters (*e.g.*, scanning speed, pulse frequency, pulse energy, overlapping rate…), various colors may be induced on the titanium surface due to oxidation.[2,12,15] Therefore, the aim of the most developed studies, conducted during the recent years both experimentally[12,13,16] and numerically,[17] was mainly the determination of the processing parameters control to obtain specific oxide growth on the marked surface, and their correlation with the color (contrast), the morphology, and the composition of the formed phases.

Although a considerable amount of papers were produced, there are substantive divergences on determining the composition of the resulting films. For instance, films produced on the same metal (CP titanium grade 4) and corresponding to the same purple color, the phases Ti, Ti_2O, TiO, and TiO_2 were obtained by Lavisse,[18] while Del Pino[13] has obtained the phases Ti, Ti_2O, and TiO.

The developed studies conducted by Lavisse *et al.*[18] concern laser marking of commercial titanium, in order to understand the influence of the laser parameters (fluence, power, pulse duration, and frequency….) and

F. BRIHMAT-HAMADI is with the Ionized Media and Laser Division, Centre de Développement des Technologies Avancées, PO. Box 17, Baba-Hassen, 16303, Algiers, Algeria, and also with Faculty of Physics, Quantum Electronic Laboratory, Université des Sciences et de la Technologie Houari Boumedienne, USTHB, BP 32 El alia Bab Ezzouar, 16111, Algiers, Algeria. Contact e-mail: fhamadi@cdta.dz E. H. AMARA is with the Ionized Media and Laser Division, Centre de Développement des Technologies Avancées, H. KELLOU is with the Quantum Electronic Laboratory, Université des Sciences et de la Technologie Houari Boumedienne, USTHB.

the environmental conditions, on formed layers contrast, morphology, structure, and chemical composition.

The developed study in reference 18 deals with the very early stage of titanium oxide formation by Nd:YAG laser beam (λ = 1064 nm and τ = 50 ns), when oxygen amount does not exceed 50 pct. By varying laser fluence in the range of 2.5 to 25 J/cm^2, various colored layers are formed on the target surface. At low laser fluences, oxidation states of obtained layers and oxygen identified with XPS analyses show that the amount of the detected Ti(II) species is about three times larger on the yellow layer than on the colorless sample. The EDX analysis confirms oxygen presence, and provides its quantity in the resulting layers. It was noted that for the yellow surface, the oxygen amount is also much larger than in the colorless layer. For the samples, treated at higher laser fluences, the obtained surfaces are purple, and more oxygen was trapped in the liquid phase. So, the various analyses indicate that the TiO oxide was not formed, knowing that the thermal model shows a solidified region.

Irradiation tests under normal atmospheric condition were also conducted by Lavisse et al.[19] to study the changes in the chemical composition of titanium surface induced by a nanosecond Nd:YAG Q-switched laser (λ = 1064 nm and τ = 35 ns), by varying the laser fluence from 4 to 60 J/cm^2. The SEM, EDS, XPS, SIMS, and Raman spectroscopy techniques have been used to analyze the formed layers. The results show that a higher fluence gives dark colors (purple and blue), rough surfaces, and crystallized TiO$_2$ phase (anatase and rutile) formation. Whereas, for low fluences, the laser passage induces smooth layers with light colors (colorless and yellow), and the XPS analysis reveals the presence of non-negligible nitrogen and oxygen in the phases.

Moreover, with the aim to understand the effect on the composition, the structure, and the optical properties of the yellow and the blue grown surface layers, Lavisse et al.[20] conducted an investigation on the influence of both laser pulse duration (5 or 35 ns) and Nd:YAG laser fluence, on the nitriding efficiency and the properties of the formed surface layers. Nuclear reaction analysis (NRA) was used to quantify the amount of light elements in the formed layers. The analysis of the results revealed that titanium oxynitrides, containing different amounts of oxygen and nitrogen, was the main finding, except in the case of long pulses and high laser fluences which led to the growth of titanium dioxide. The thickness of the surface layers determined by electron microscopy observations shows that a high thickness is obtained on the blue surface treated with long pulse duration. 3D optical profilometer was also used to analyze the roughness of the obtained layers. The authors show that the roughness is sensitive to pulse duration: layers obtained with short pulse duration have smaller roughnesses than those obtained with longer duration. This observation has been explained by modeling the Nd:YAG laser interaction with titanium,[21] and an evaporation regime is produced in the case of short pulses, whereas a mixed liquid-ablation regime is found for the longer pulses, where a solidified melt leads to higher surface roughness.

Furthermore, with constant pulse duration, the roughness increases with laser fluence.

In addition to the studies held in order to determine the main reasons for surface coloration, several studies have also been carried out to determine the effect of the parameters on the coloration and the films' chemical composition. Adams et al.[15] studied using nanosecond fiber laser (1064 nm) color marking of CP grade 2 Ti. X-ray diffraction electron microscopy was used to evaluate the phases formed in color films in order to develop a better understanding of how the structure and the composition of laser-grown films affect colored appearance. In their investigation, they revealed that coatings are titanium monoxide TiO and the differences in color are likely the result of variations in the TiO films' thicknesses. Controlling the laser parameters allows controlling the extent of localized laser heating and provides more control over oxide thickness, phase, and quality. Adams et al.[16] also conducted a study on laser marking using a Nd:YAG (1064 nm) nanosecond pulsed laser under air environment on polished titanium. Detailed microstructure and phase analysis showed that coatings generally consist of three layers. A thin layer of TiO$_2$ rutile was formed at the surface of coatings, and at the bottom, a cubic TiO is formed. This crystalline, middle layer contained only traces of N and appeared to have a uniform composition, whereas, the bottom layer consisted of an inhomogeneous mixture of Ti, O, and N. The phase in this sub-surface volume was identified as TiO$_x$N$_{1-x}$. Whereas, Del Pino et al.[12] show the formation of a complex mixture of oxygen-rich phases of TiO$_2$, Ti$_2$O$_3$, TiO, and Ti$_2$O as a result when a nanosecond laser irradiation interacts with titanium (grade 4) in air using a high laser fluence. A similar study conducted by Langlade et al.[22] treated commercially pure titanium with a pulsed Nd:YAG laser in ambient air. The authors found a range of titanium oxides and concluded that although the layer thickness may have an effect, the different colors they observed corresponded to different titanium oxides.

Measurements and analyzes of the marking parameters influence on the colors obtained on titanium by pulsed fiber laser were performed by Arkadiusz et al.[23] whereas Skowronskia et al.[24] proposed a study of the chemical composition and the optical spectra of titanium films formed under air environment, during irradiation by a pulsed Yb: Glass fiber laser. The authors noted a presence of titanium dioxide on the top layer of the formed film and reduced titanium oxides and/or oxynitrides in the sub-surface layer.

Due to the important number of the involved laser parameters (pulse energy, pulse duration, frequency, scanning speed, line spacing, gas environment, etc), which may affect the state of the treated surface, a huge number of experiments must be performed. However, the number of necessary experiments with identified process parameters can be reduced using a design of experiment method (DOE). Some studies have been carried out using Nd:YAG laser in order to determine the effect of the process parameters on the surface roughness, the surface reflectance, the mark contrast, and the removed material depth. Soveja et al.[25] used

the DOE to investigate the effect of the repetition rate, the pulses energy, the scanning speed, and the line spacing, on the marked surface roughness, on the material removal rate, and on the composite function. The results analysis showed that only the frequency and the pulses energy, among the studied influencing factors, have a significant influence on laser surface texturing process. A similar study was conducted by Ibrahim et al.[26] to investigate the micro-milling performance of the AISI H13 with different processing parameters, namely laser power, scanning speed, frequency, and fill spacing. Using a 30W fiber laser marking machine, they found the optimal operating conditions for minimum surface roughness and maximum milling depth. For all experiments, the surface roughness and milling depth depends on laser scan speed and laser power. The surface roughness decreases with decreasing the laser power and the pulses frequency, when the surface is machined at high scan speed. The milling depth increased with the decreasing of scan speed and fill spacing. However, a lower value of scan speed and fill spacing decreased the surface roughness. Campanelli et al.[27] used a DOE method to study the influence of the laser fluence and the degree of overlap on the removed material depth and surface roughness when samples are treated by nanosecond Nd:YAG laser source. The obtained results show that roughness is generally opposite to the depth result. The degree of overlap affects significantly the surface roughness, where its highest values were observed for higher degrees of overlap. Moreover, the analysis of laser fluence suggested that the highest values of the material removal rate correspond to the highest values of laser fluences. The results show that roughness values are constant; they do not vary with the laser fluences for lowest scanning speed values, whereas for larger scanning speed the surface roughness increases by increasing the laser fluence.

In most of the works on laser marking of titanium and its alloys, the roughness, the reflectance, and the phases composition were discussed by some authors,[12,16,20,25,28,29] but none of them presented a clear correlation between all the characteristics of the treated surface (roughness, reflectance, contrast, and chemical composition).

In the present paper, the developed work concerns an experimental part performed in the "Laboratoire Inter-disciplinaire Carnot de Bourgogne" Bourgogne University (France). It constitutes a continuation of the work performed by Lavisse et al., which did not address the effect of the operating parameters on the roughness of the treated surface. Following our study results, higher roughness of surface leads to a lower reflectance. This occurs when high laser fluences or lower scan speeds are used. Therefore, our main objective is to find the optimal operating conditions for minimum surface roughness and maximum surface reflectance. We develop a study of the titanium surface contrast change, characterized by its reflectance in the visible range, its roughness, and its chemical composition when it is exposed to nanosecond Nd: YAG laser radiation.

II. DETAILS OF THE EXPERIMENT

A. *The Laser Beam*

The laser choice is guided by the possibility of obtaining marked patterns depending on the whole material physical properties. In this work, a Q-switched and frequency-doubled Nd:YAG green laser (KALUTI) operating at 532 nm and delivering 5 ns pulse duration is used. The focused laser spot moves with a galvano-metric scan mirrors that allow the beam to be deflected over the titanium substrate surface with a constant velocity to form parallel straight lines. All experimental tests are obtained using a Gaussian circular laser spots, with a maximum energy per pulse of 0.3 mJ corre-sponding to an average power per pulse equal to 30 W, at a repetition rate of 100 kHz. The laser beam is focused by a 160 mm focal length lens, giving an average focal spot diameter of about 40 μm on the substrate surface. The process parameters and the motion of the laser beam over the substrate were controlled by a personal computer and Mark software.

B. *The Sample*

The used substrate is commercial pure (CP) titanium (grade 4) with dimensions of 10 mm × 10 mm × 2 mm. Before starting the marking, the sample's surface was mechanically polished till 1200 paper grade to obtain a roughness less than 0.3 μm, and then it is cleaned with ethanol. Circular marks of 9 mm diameter are realized on the prepared samples.
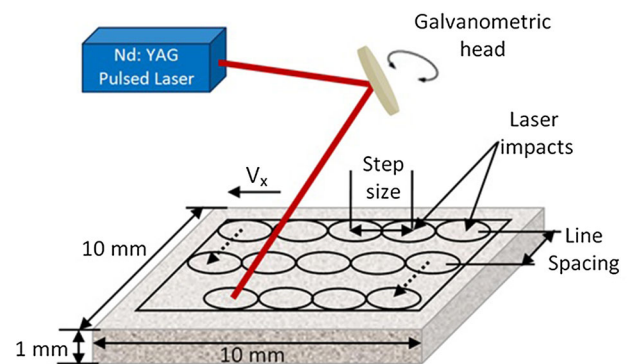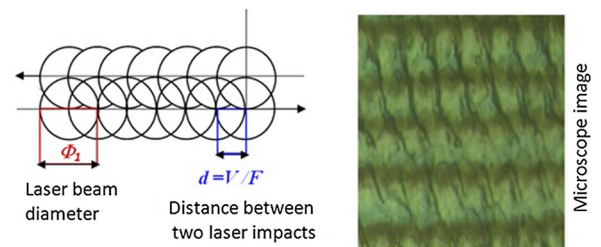

Fig. 1—Schematic representation of the laser marking.

C. Experimental Procedure

During the laser marking process, the focused beam moves over the metallic surface and when absorbed, it produces a thermal reaction within the interaction zone. According to a forward and a backward motion, passes separated by a fixed line space are induced, and as shown on Figure 1, they form series of parallel segments covering a part of the sample surface. The distance between two consecutive laser pulses is related to the scanning speed (V) and to the repetition rate (f), which govern the lateral overlap (x direction) of the irradiated surface. The overlapping rate can be calculated by the following equation[26,27,30]:

$$\text{OR} = \left(1 - \frac{V}{f \times \Phi}\right) \times 100 \qquad [1]$$

Table I gathers the frequency f (Hz), the scanning speed V (mm/s), and the pumping intensity I (A) values of the different laser treatment parameters used in this work. The parameter P_a (W) is implicitly calculated from I (A). E_p (J) and F_p (J/cm^2) are deduced from the average laser power and are used in Eq. [2] to calculate the accumulated fluences F_{acc} (J/cm^2). The corresponding values of F_{acc} and the laser fluence per pulse F_p (J/cm^2), given in Table I, can be calculated by taking into account the laser fluence per pulse F_p and the total number of pulses N_P following the relations[31]:

$$F_p = \frac{4 \times P_a}{\pi \times \Phi^2 \times f}, \quad N_P = \frac{\pi \times \Phi^2 \times f}{4 \times V \times d} \qquad [2]$$

$$F_{acc} = F_p \times N_P = \frac{P_a}{V \times d} \qquad [3]$$

P_a(W) is the average laser power and $d(\mu m)$ the line spacing. The overlapping rate OR(pct) shown in Table I, is deduced from Eq. [1] for different values of the pulse frequency f (s^{-1}) and the scanning speed V(mm s^{-1}). E_P(J) is the laser energy per pulse and $\Phi(\mu m)$ is the laser spot diameter.

$$E_P = \frac{P_a}{f}. \qquad [4]$$

D. Techniques of Characterization

The treated surfaces are characterized by performing measurements using a profilometer and a colorimeter to obtain direct values of the roughness average Ra in micrometers and colorimetric properties represented by CIELab coordinates C^*, a^*, and b^*, in order to locate a color in the chromaticity diagram. A Veeco–Wyko NT 9100 profilometer is used, assisted by the Vision software to analyze the surface roughness. The colorimetric measurements of the treated surfaces are recorded using a Konica Minolta CM 3500d universal colorimeter, including a D65 lamp. The data were processed with the SpectraMagic software, which provides color values by rational numbers (a*, b*, and C*). We obtain spectral reflectance graphs according to the wavelength in the visible range (400 to 700 nm) for different layer of colors. The microscope photos and the measurements of roughness were carried out with a confocal optical microscope. The chemical composition analysis of the samples processed by different laser parameters, with θ to 2θ geometry was performed by X-ray diffraction (Siemens D5000 diffractometer, $\lambda = 1.5406$ A) at 40 kV and at 30 mA. After the treatment of the surfaces, the elemental analysis of the formed colors was obtained by energy-dispersive X-ray spectroscopy (EDS–EDAX) system integrated with the SEM unit. The colors, surface roughness, and colorimetric properties of the layers are listed as output variables in Table II.

III. RESULTS AND DISCUSSION

A. Optical Images of Marks

Figure 2 reveals the effect of the laser beam parameters on the marking quality, where optical microscope images showing the morphology of the formed layers are reported. It can be observed that the titanium surface morphologies are very sensitive to the overlapping rate OR[27] and to the accumulated laser fluence.[19,28] At a low frequency and a high scanning speed (A3 test), the effect of each laser pulse along the mark is very weak, and the observed cracks shown on A3, B3, and C3 tests are related to the formation of the oxides in the alpha phase. By increasing frequency, as shown on

Table I.   Input Variables

| Variables	A1	A2	A3	B1	B2	B3	C1	C2	C3
f (kHz)	5	5	5	10	10	10	20	20	20
V (mm/s)	5	50	200	5	50	200	5	50	200
I (A)	24.05	25.90	29.60	24.05	25.90	29.60	24.05	25.90	29.60
P_a (W)	0.75	1.00	1.25	0.90	1.10	1.55	1.10	1.20	1.80
E_p (mJ)	0.150	0.200	0.250	0.090	0.110	0.155	0.055	0.060	0.090
F_p (J/cm^2)	11.90	15.90	19.90	7.16	8.75	11.94	4.40	4.80	7.20
N_P	84	14	2	168	28	4	335	56	8
F_{acc} (J/cm^2)	1000	222.3	41.7	1201	244.5	50	1464	266.8	60
OR (pct)	97.50	85.00	00.00	98.75	92.50	50.00	99.37	96.25	75.00
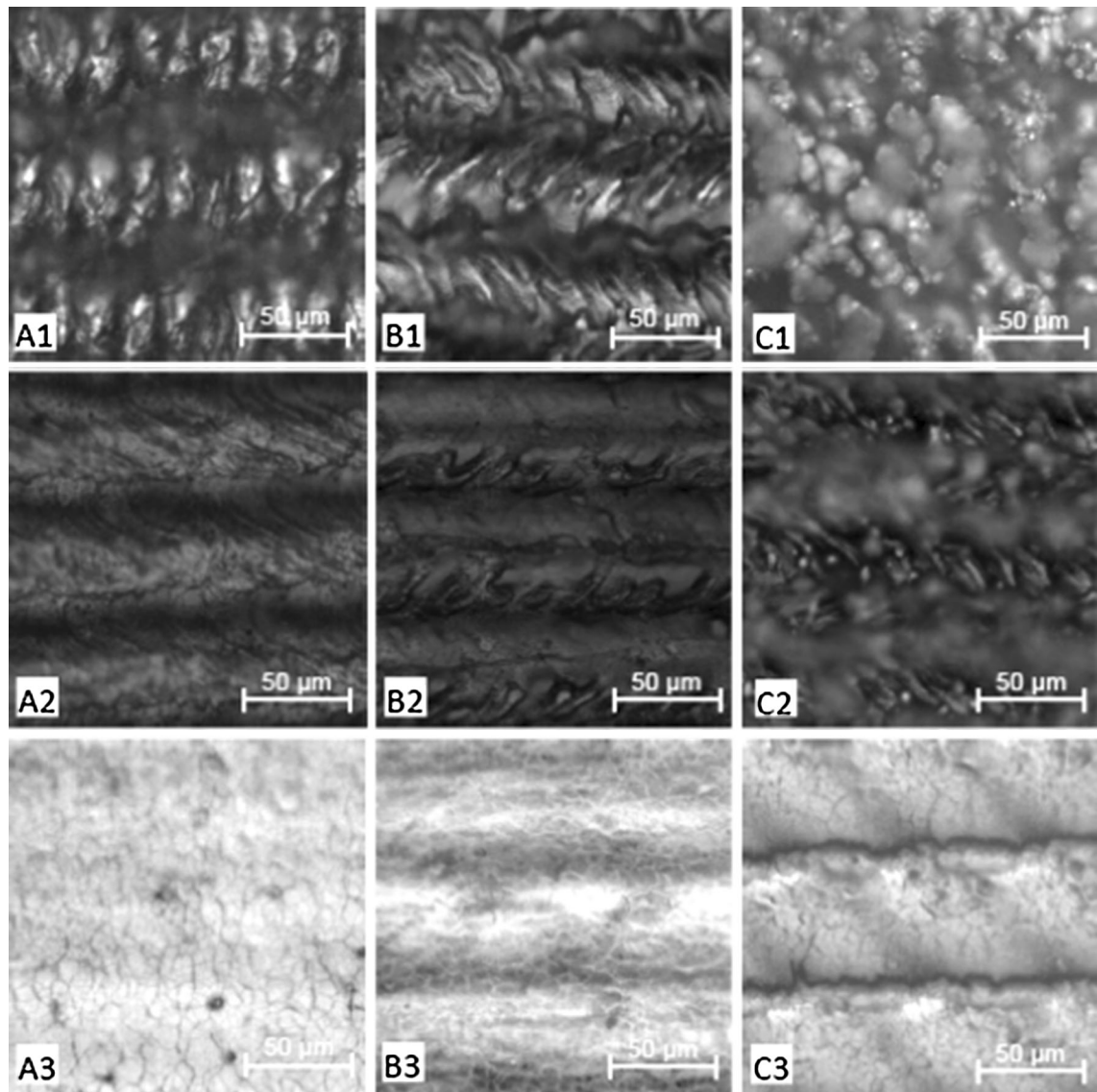
Fig. 2—Microscope images of the formed layers on titanium substrate at various processing parameters (see Table I).

C3 test, a higher density of striations is obtained, resulting from the overlapping of a larger number of impacts per unit mark length. Further decreasing of the scanning speed leads to the increasing of the striation density, resulting in a darker mark surface. The scanning speed and the laser pulse frequency which determine the overlapping of laser impacts (corresponding to the number of superimposed pulses on the same area) as given in Eq. [1], affect the surface temperature when the overlap rate becomes higher.

Indeed, we note that the marking contrast decreases rapidly when decreasing the overlapping rate and the accumulated laser fluences, as indicated by the corresponding results of the color digital data listed in Table II. It is clearly shown that the contrast of the three samples of the series C is darker than that of the samples of the series B and A.

B. *Profilometry*

The 3D optical profilometer measurement results obtained on the layers surface processed by laser are shown in Figure 3. The pictures show the variation of the surface roughness of the test samples. They revealed gradual laser-induced effects at different accumulated laser fluences, which were caused by the fast melting and solidification processes, knowing that the melting fluence threshold (~4.2 J/cm^2) is far exceeded.

For all the accumulated fluences, it is observed that a rough surface varies from a high surface roughness Ra (Table II) to a smoother one, depending on the accumulated laser fluences and on the overlapping rate values. The results indicate also that, for a fixed value of the scanning speed (Table I), the increasing of the accumulated laser fluences causes an increase in the energy per unit area, and

Table II. Output Variables

Variables	A1	A2	A3	B1	B2	B3	C1	C2	C3
Color	Brown	light brown	light yellow	dark green	light brown	Yellow	darkblue/purple	blue	yellow
Ra (μm)	0.70	0.41	0.32	0.74	0.64	0.5	1.12	1.02	0.6
C*	8.36	36.76	4.91	6.82	21.54	17.49	5.66	17.80	19.73
a*	−7.54	8.82	0.22	−2.00	5.99	1.93	5.26	1.55	3.21
b*	−3.63	35.69	4.91	−6.53	20.7	17.39	−2.11	−17.74	19.47
Chemical composition (θ to 2θ geometry)	Ti (α), Ti$_2$O$_{(hc)}$, TiO$_{cfc}$	Ti (α), Ti$_3$O$_{(hc)}$, Ti$_2$O$_{(hc)}$, TiO$_{cfc}$	Ti (α), Ti$_3$O$_{(hc)}$, Ti$_6$O$_{(hc)}$	Ti (α),TiO$_{cfc}$, TiO$_{2\,(m)}$, TiO$_{2(hc)}$	Ti (α), Ti$_3$O$_{(hc)}$, Ti$_2$O$_{(hc)}$, TiO$_{cfc}$	Ti (α), Ti$_6$O$_{(hc)}$, Ti$_3$O$_{(hc)}$, Ti$_2$O$_{(hc)}$	Ti(α),Ti$_2$O$_{3(rh)}$, TiO$_{cfc}$,TiO$_{2(m)}$, TiO$_{2(hc)}$, γ-TiO$_2$	Ti(α),TiO$_{2(hc)}$, Ti$_2$O$_{3}$ (rh), TiO$_{2(m)}$, TiO$_{2(hc)}$	Ti (α), Ti$_6$O$_{(hc)}$, Ti$_3$O$_{(hc)}$, Ti$_2$O$_{(hc)}$

consequently leads to an increase of the surface roughness by the formation of the most prone grooves. As illustrated in Figure 3, the images show that, the test samples of the series A, B, and C, treated with an overlap greater than 90 pct exhibit a higher surface roughness and the obtained values show that the roughness Ra of the A series is lower compared to the B and C series.

For all the test samples of the A, B, and C series, the surface profile of the laser pass according to x axis reveals several peaks with a height of 0.5 to 1 μm formed after the re-solidification of the molten material. For the high value of laser impacts overlapping rate, when the accumulated fluences are increasing, the 2D plots of the surface profile are characterized by very high peaks. Conversely, at higher scanning speed 200 mm/s [low OR (pct)], the height of the peaks is around 0.3 μm, and a net increase in the roughness with increasing overlapping rate occurs as shown for the A1, B1, and C1 tests.

C. X-ray Diffraction Results

The analysis of the processed surface by X-ray diffraction (XRD) is needed in order to know the nature of the chemical composition of the produced marks for the three series of the treated titanium at different conditions.

Figure 4 represents the obtained XRD results for the all treated samples; we note that different phases are formed on titanium surface by modifying each of the accumulated laser fluence, the scanning speed, and the laser frequency.[5,20,32]

During the laser titanium interaction, the thermal effects result in surface heating, but can also get to a molten and vaporized material. In addition, as mentioned in the Eq. [3], the accumulated laser fluence depends strongly on the scanning speed of the laser beam displacement. By analyzing the produced phases on all tests against the laser fluence, some conclusions can be drawn: the intensity of titanium in its α phase Ti(α), decreases as the accumulated laser fluence increases, and on the other hand, the increasing of accumulated laser fluence causes an increasing in the oxidation state of the metallic titanium. In the majority of the tests having a dark color, the measurements always reveal the formation of a mixture of several titanium oxides TiO, Ti$_2$O$_3$, and TiO$_2$ (rutile, anatase, and γ phases), which appear in the cases when the accumulated laser fluence exceeds 1000 J/cm^2. The XRD patterns of A3, B3, and C3 tests treated at lower accumulated laser fluences indicate that, the identified titanium oxides (Ti$_6$O, Ti$_3$O, and Ti$_2$O) have lower oxidation degrees. Their formation is due to the oxygen diffusion in the α titanium lattice.

It is remarked also that the maximum accumulated fluences of 1000, 1200, and 1464 J/cm^2 used in the most roughened surfaces of the A1, B1, and C1 tests, respectively, were sufficient to produce different phases on titanium surface. The obtained oxidized phases are TiO (JCPDS-90-220) cubic crystallographic structure with centered faces (FCC), Ti$_2$O$_3$ (JCPDS71-1046), TiO$_2$ anatase (JCPDS-71-1168), TiO$_2$ rutile (JCPDS-053-0326), and γ-TiO$_2$ (JCPDS-053-0619). These results
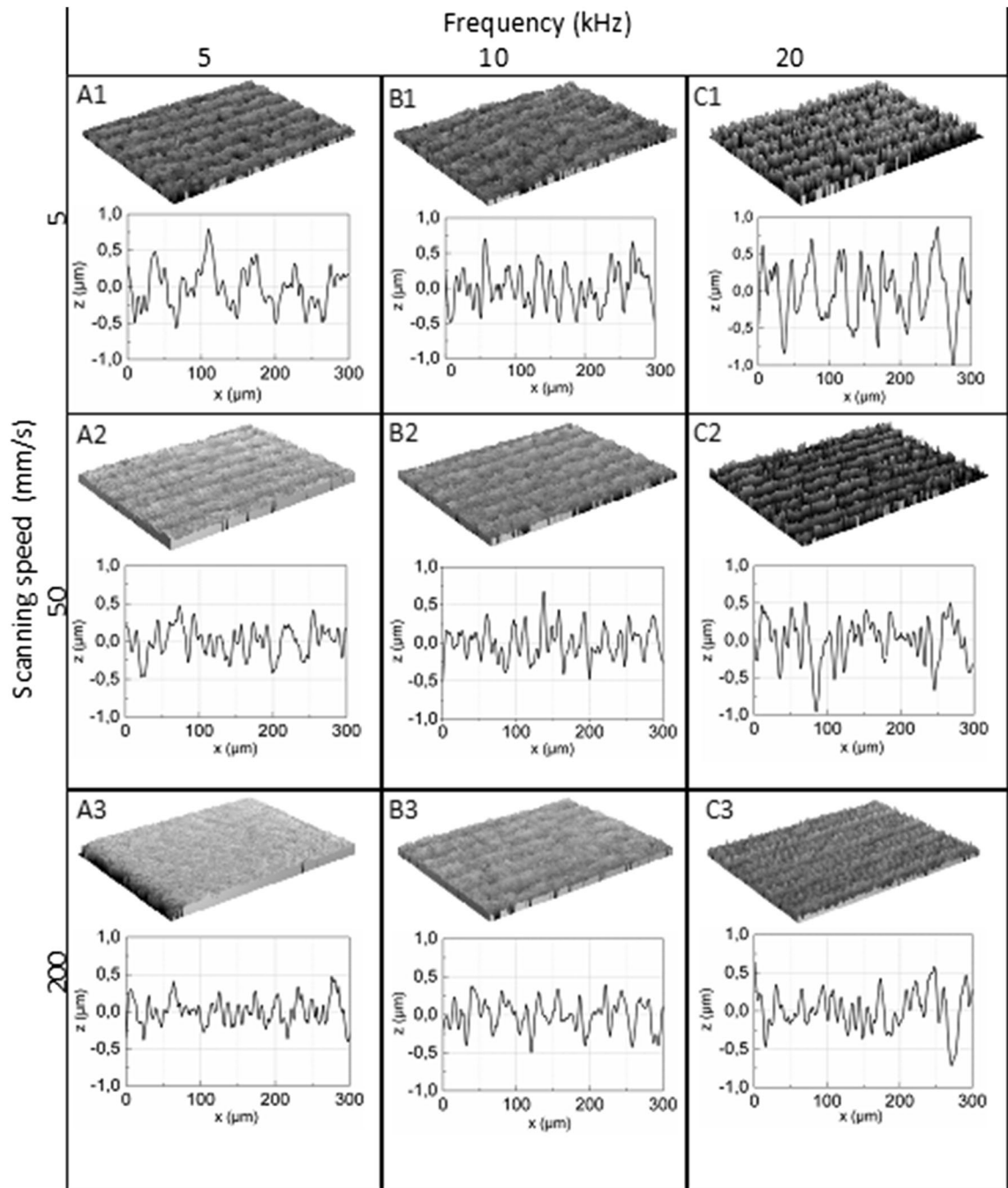
Fig. 3—3D surface profile roughness and 2D plot x axis of surface profiles.

were obtained by some authors[13,33] who have shown that the higher accumulated fluence causes a higher degree of oxidation, *i.e.*, with high oxygen diffusion, samples will trap more oxygen in the solidified phase of the melt. From the Figure 4, it can also be observed that for each series as the accumulated fluence is increased, there is a decrease in the signal of α-Ti phase and an increase in the intensity signal of the face-centered cubic TiO (200), located at 2θ (deg) = 43,37 deg. It is important to note that even for the surfaces modified with the same scanning speed, the samples present different surface phase distribution depending on the

accumulated laser fluence and on the overlapping rate of laser impacts. In addition, the yellow layers contain oxides corresponding to the chemical formula of Ti_nO (n = 1, 2, 3, and 6). The brown, purple, and blue layers formed on the titanium surface with high accumulated laser fluence (highest overlapping rate) contain highly oxidized compounds of Ti_2O_3 and TiO_2.

The XRD results corresponding to the test B1 showed that beyond its laser accumulated fluence (above 1200 J/ cm^2), the TiO_2 anatase (101) phase becomes dominant while a weak characteristic signal of TiO_2 rutile (110) and γ-TiO_2 (orthorhombic) appears. It is found that the
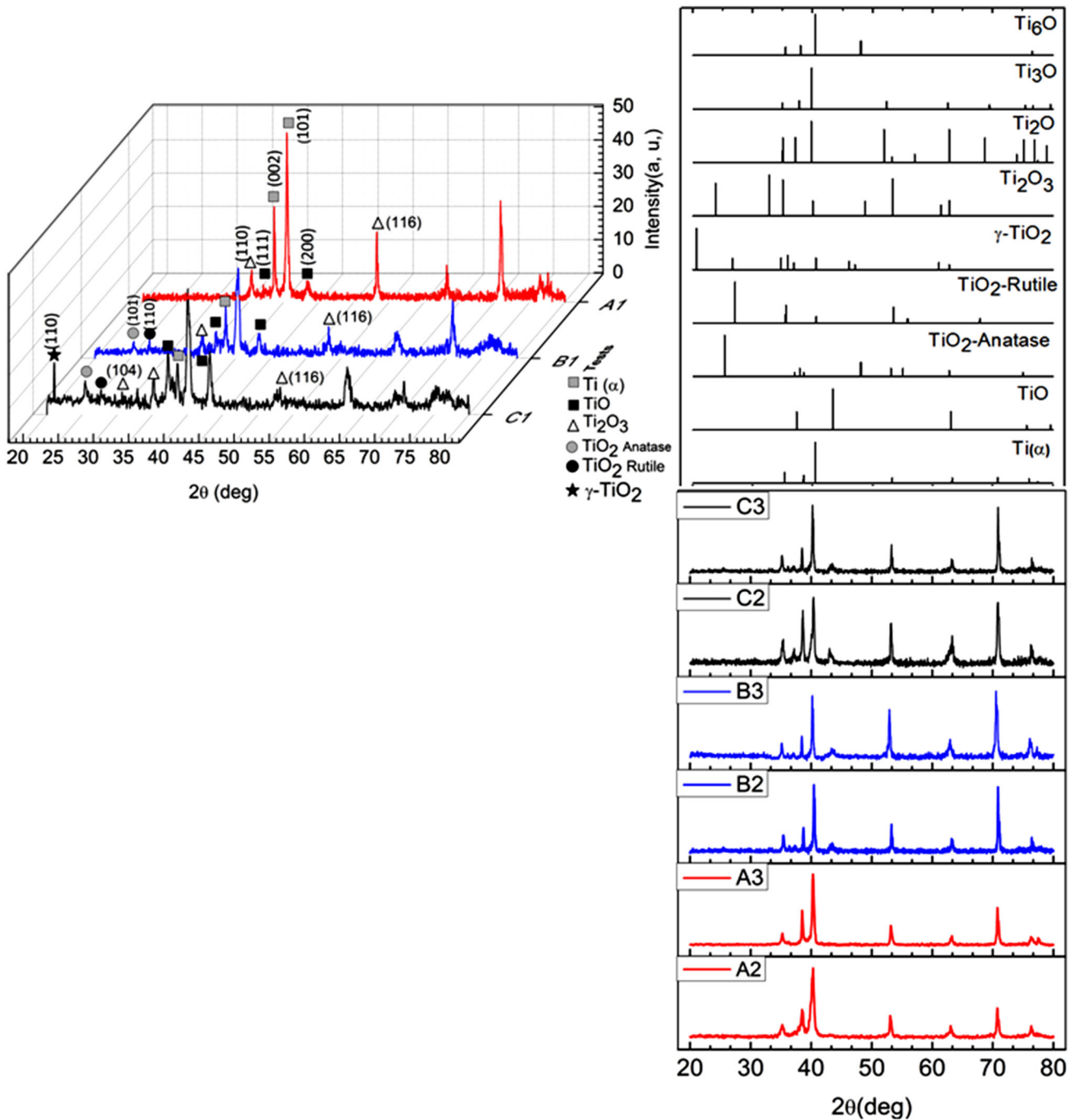
Fig. 4—X-ray diffraction patterns of titanium treated by laser obtained for tests cited in Table I, with the powder diffraction patterns corresponding to α-Ti, Ti_3O, Ti_6O, Ti_2O, TiO, TiO_2 (rutile, anatase, and γ phases), and Ti_2O_3.

surfaces treated with low fluences show no peak of oxides. In contrast, the diffraction peak is visible for stronger laser fluences. Moreover, the results show for the darkest layer corresponding to the test C1, treated with the maximum accumulated laser fluence, a presence of a diffraction peak located at 2θ (deg): 20.60 deg corresponding to the plane reflections (110) of γ-TiO_2 orthorhombic structure. However, the intensity of the Bragg diffraction attributed to TiO_2 rutile phase (110) tetragonal structure located at 27.05 deg becomes low, compared to the intensity shown in the test B1. The

XRD analysis shows also that for low fluences ($F_{acc} <$ 1000 J/cm^2), the laser treatment induces yellow films composed of phases with low oxidation degrees Ti_6O, Ti_3O, Ti_2O, TiO, and Ti_2O_3. Two weak peaks that could be attributed to Ti_2O_3 located at 2θ (deg): 34.96 deg and 53.22 deg appear in the samples C2 obtained at intermediate accumulated laser fluence 266.8 J/cm^2 and for the realized treatments C1, with high fluences $F_{acc} >$ 1200 J/cm^2.

We proceeded to further identification of the phases present in the colored layers using energy-dispersive
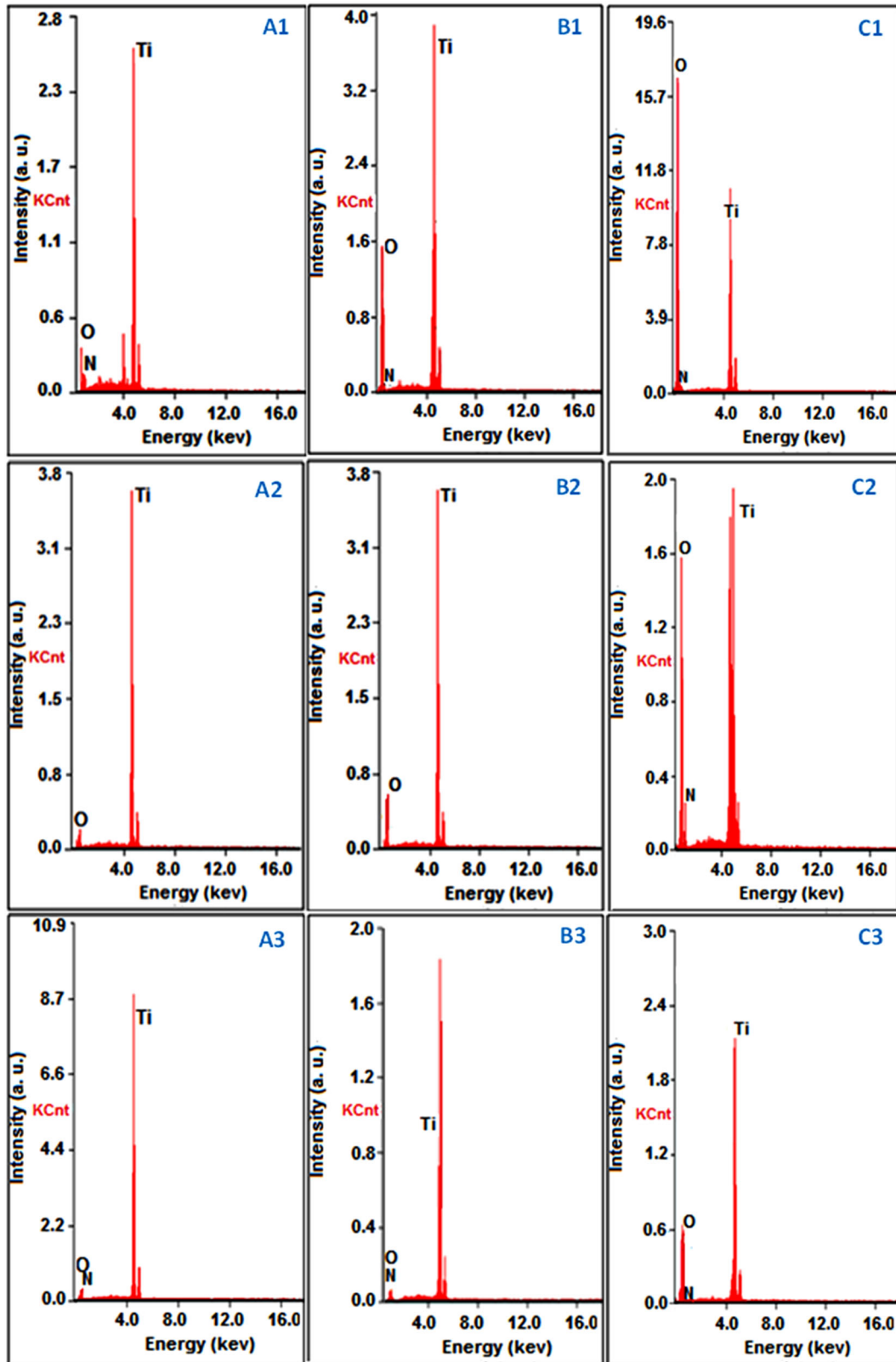
Fig. 5—EDS analysis of obtained layers after the laser treatment of titanium.

X-ray Spectroscopy (EDS) to assay the difference in the composition of the thermal oxidized titanium substrate. The semi-quantitative results of the chemical surface composition obtained for individual points are reported in Figure 5. Two categories corresponding to high and low accumulated laser fluences of the treated samples

Table III. Chemical Composition of Layers After the Laser Treatment of Titanium

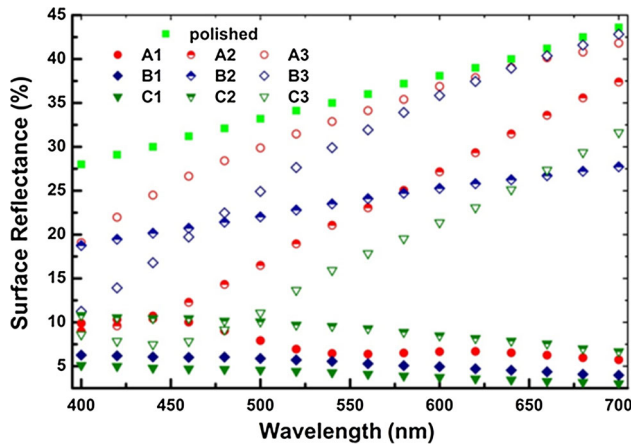| Sample	Elements Weight Percent		
	Ti K	O K	N K
A1	70.55	20.01	9.44
A2	78.06	18.60	3.34
A3	91.14	5.26	3.60
B1	63.81	33.32	2.87
B2	71.96	25.96	2.08
B3	82.97	10.44	6.59
C1	41.35	56.61	2.04
C2	50.37	43.52	6.11
C3	74.32	22.70	2.98

Fig. 6—Reflectance spectrum of sample surfaces at different processing conditions, with the spectrum of the untreated substrate.

are reported. As found in literature, when titanium is exposed to the oxygen contained in the atmosphere, it results in the formation of an oxide layer.[12,13,15,16,19] This formation is more pronounced when the substrate is heated above melting temperature since it results in fast insertion of the atmospheric air element.

The EDS results demonstrate a decreasing trend for oxygen level on the layers, when the accumulated laser fluences and overlapping rate decrease.

Based on the EDS analysis of the obtained colors, it is clear that, even at lower laser accumulated fluences (A2, A3, B2, B3, C2, and C3), the oxygen content is exceeding the nitrogen content, because titanium metal is highly reactive and has an extremely high affinity for oxygen. But when the substrates are strongly heated, by decreasing the scanning speed, it results in an increased overlapping rate and accumulated laser fluences. EDS analysis of the dark layers shows high amount oxidation with its weight percent at 56.53 (C1 test). The oxygen peak appears clearly, and this allows to confirm that an oxidation phenomenon has indeed occurred, and that the resulting oxide layer is responsible for the color appearance. The EDS spectrum obtained for samples treated at low scanning speed shows an important peak of oxygen. Table III summarizes the results of analysis

of the chemical composition of the different marked zones.

Figure 6 presents reflectance spectrum of sample surfaces at different processing conditions in the normal air ambiance. Compared with bare Ti, all formed oxide films exhibit a decreased reflectance for all specified wavelengths. The treated samples with low accumulated laser fluences, having a low coloration contrast (yellow and green layers) show a high reflectance percentage, throughout the visible part of the electromagnetic spectrum. The treated area on the samples reflects 25 to 40 pct of the incident light resulting in a 700 nm radiation (red light), and shows no significant difference on the surface reflectance curve tendency compared to the untreated polished parts of the sample for the A2, A3, B2, B3, and C3 tests.

It is worth to note that for the same scanning speed, the reflectance in the visible spectrum (400 to 700 nm) increases with the decreasing of the laser accumulated fluence. In contrast, for the samples treated with the maximum fluence (A1, B1, and C1), we note that their surfaces are very rough (see Figure 3), consequently they negatively affect the reflectance of incident white light giving very low values in the visible spectrum between 5 and 10 pct.

We can note that the reflectance spectra of the sample A1, treated at 1000 J/cm^2, is a mixture of the blue, red, and yellow colors, consequently leading a dark brown color. It can be observed that a varying spectral reflectance is exhibited, and it is characterized by maxima and minima corresponding to the wavelengths 425, 562, and 630 nm.

In addition, using reflectance spectrum, a distinction can be made between same colored layers, especially concerning B1 and C1 layers, which were treated with higher laser accumulated fluences, at high overlapping rate of the laser impacts. It is noticed from Figure 6, that the reflectance is lowest, and this is due to the fact that the surface has become more granular. As the surface becomes more granular with the increasing of the overlapping rate of laser impacts, the light is more scattered or absorbed causing destructive interferences or dark colors. With the reduced number of laser pulses, the laser-treated area is less granular and therefore light is less scattered or more reflected causing constructive interferences or bright colors (e.g., yellow brown and light green).

IV. CONCLUSION

This work is part of a global study on the characterization of colored titanium surfaces formed using a laser marking with short pulse duration.

– The characterization of oxide layers developed using a laser beam in pulse mode shows the presence of various oxide functions of accumulated laser fluence.
– The treated surfaces with accumulated laser fluence greater than 1000 J/cm^2 are more affected. They are characterized by: dark contrasts, high oxidation state of titanium atoms (+IV) of the formed phases, high

roughness caused by the formation of the grooves, and low reflectance.
– Using high accumulated laser fluence, several TiO_2 structures have been observed: anatase, rutile, and another phase having orthorhombic structure, has been identified (Figure 4).
– For low accumulated laser fluences, the laser passage onto the surface induces smooth surface layers and light colors. XRD spectra reveal the presence of low oxidized titanium atoms.
– Increasing the overlapping rate by decreasing the laser scanning speed increases the temperature of treated region.
– The correspondence between the observed results indicates that there is some correlation between the color and phase composition (XRD spectra). A complete correlation of the color and composition cannot be declared, as for the very similar two colors of B1 and C1 layers don't present the same XRD spectrum.

REFERENCES

1. K. Mahmood, N. Farid, I.M. Ghauri, N. Afzal, Y. Idrees, and F.E. Mubarik: *Phys. Scripta*, 2010, vol. 82, p. 045606.
2. Ryo. Honda: *Int. J. Mod. Phys.*, 2012, vol. 6, pp. 682–87.
3. Z.L. Li, H.Y. Zheng, K.M. Teh, Y.C. Liu, G.C. Lim, H.L. Seng, and N.L. Yakovlev: *Appl. Surf. Sci.*, 2009, vol. 256, pp. 1582–88.
4. P. Deprez, C.F. Melian, F. Breaban, and J.F. Coutouly: *J. Surf. Eng. Mater. Adv. Technol.*, 2012, vol. 2, pp. 32–39.
5. A. Peréz Del Pino, P. Serra, and J.L. Morenza: *Appl. Surf. Sci.*, 2002, vols. 197–198, pp. 887–90.
6. H. Takikawa, T. Matsui, T. Sakakibara, A. Bendavid, and P.J. Martin: *Thin Solid Films*, 1999, vol. 348, pp. 145–51.
7. K.S. Teng, J.L. Delplancke, J. Zhang, and T.J. O'keefe: *Metall. Mater. Trans. B*, 1998, vol. 29B, pp. 749–54.
8. J.M. Lackner, W. Waldhauser, R. Ebner, B. Major, and T. Schoberl: *Surf. Coat. Technol.*, 2004, vol. 180, pp. 585–90.
9. R. Pandian, G. Natarajan, S. Rajagopalan, M. Kamruddin, and A.K. Tyagi: *Appl. Phys. A*, 2014, vol. 116, pp. 1905–13.
10. H. Dong and T. Bell: *Wear*, 2000, vol. 238, pp. 131–37.
11. C.E.B. Marino, E.M. de Olivera, R.C. Rocha-Filho, and S.R. Biaggio: *Corros. Sci.*, 2001, vol. 43, pp. 1465–76.
12. A. Peréz Del Pino, J.M. Fernandez-Pradas, P. Serra, and J.L. Morenza: *Surf. Coat. Technol.*, 2004, vol. 187, pp. 106–12.
13. L. Lavisse, C. Langlade, P. Berger, D. Grevey, and A.B. Vannes: *Mater. Sci. Forum.*, 2004, vols. 461–464, pp. 697–704.
14. S. O'Hana, A.J. Pinkerton, K. Shoba, A.W. Gale, and L. Li: *Surf. Eng.*, 2008, vol. 24, pp. 147–53.
15. D.P. Adams, R.D. Murphy, D. Saiz, M. Rodriguez and D. Hirschfeld: CLEO, OSA. 2013, CM1H.7.pdf.
16. D.P. Adams, R.D. Murphy, D.J. Saiz, D.A. Hirschfeld, M.A. Rodriguez, P.G. Kotula, and B.H. Jared: *Surf. Coat. Technol.*, 2014, vol. 248, pp. 38–45.
17. J.L. Jiménez Pérez, P.H. Sakanaka, M.A. Algatti, J.G. Mendoza-Alvarez, and A.C. Orea: *Appl. Surf. Sci.*, 2001, vol. 175, pp. 703–08.
18. L. Lavisse, D. Grevey, C. Langlade, and B. Vannes: *Appl. Surf. Sci.*, 2002, vol. 186, pp. 150–55.
19. L. Lavisse, J.M. Jouvard, L. Imhoff, O. Heintz, J. Korntheuer, C. Langlade, S. Bourgeois, and M.C. Marco de Lucas: *Appl. Surf. Sci.*, 2007, vol. 253, pp. 8226–30.
20. L. Lavisse, P. Berger, M. Cirisan, J.M. Jouvard, S. Bourgeois, and M.C. Marco de Lucas: *J. Phys. D*, 2009, vol. 42, p. 245303.
21. V. Semak and A. Matsunawa: *J. Phys. D: Appl. Phys.*, 1997, vol. 30, pp. 2541–52.
22. J.R. Krafft and J.R. Martin: *Surf. Coat. Technol.*, 1998, vol. 100, pp. 383–87.
23. A.J. Antonczak, B. Stepak, P.E. Kozioł, and K.M. Abramski: *Appl. Phys. A*, 2014, vol. 115, pp. 1003–13.
24. L. Skowronski, A.J. Antonczak, M. Trzcinski, L. Lazarek, T. Hiller, A. Bukaluk, and A.A. Wronkowska: *Appl. Surf. Sci.*, 2014, vol. 304, pp. 107–14.
25. A. Soveja, E. Cicala, D. Grevey, and J.M. Jouvard: *Opt. Laser Eng.*, 2008, vol. 46, pp. 671–78.
26. E.I. Saklakoglu and S. Kasman: *Int. J. Adv. Manuf. Technol.*, 2011, vol. 54, pp. 567–78.
27. S.L. Campanelli, G. Casalino, and N. Contuzzi: *Opt. Laser Technol.*, 2013, vol. 52, pp. 48–56.
28. E. Akman and E. Cerkezoglu: *Opt Lasers Eng.*, 2016, vol. 84, pp. 37–43.
29. D. Du, Y.F. He, B. Sui, L.J. Xiong, and H. Zhang: *J. Mater. Proc. Techol.*, 2005, vol. 161, pp. 456–61.
30. W. Pacquentin: Contribution à l'étude des propriétés physico-chimiques des surfaces modifiées par traitement laser. Thèse de Doctorat, Université de Bourgogne, France, 2011.
31. F. Torrent: Fonctionnalisation de surfaces métalliques par des couches minces d'oxynitrures de titane obtenues par irradiation laser sous atmosphère contrôlée et par PVD. Thèse de Doctorat, Université de Bourgogne, France, 2013.
32. F.J.C. Braga, R.F.C. Marques, E.A. Filho, and A.C. Guastaldi: *Appl. Surf. Sci.*, 2007, vol. 253, pp. 9203–11.
33. L. Nanai, R. Vajtai, and T.F. George: *Thin Solid Films*, 1997, vol. 298, pp. 160–64.